Determination of Stress Parameters for Eight Well-Recorded Earthquakes in Eastern North America

by David M. Boore, Kenneth W. Campbell, and Gail M. Atkinson

Abstract   We determined the stress parameter, $\Delta\sigma$, for the eight earthquakes studied by Atkinson and Boore (2006), using an updated dataset and a revised point-source stochastic model that captures the effect of a finite fault. We consider four geometrical-spreading functions, ranging from $1/R$ at all distances to two- or three-part functions. The $\Delta\sigma$ values are sensitive to the rate of geometrical spreading at close distances, with $1/R^{1.3}$ spreading implying much higher $\Delta\sigma$ than models with $1/R$ spreading. The important difference in ground motions of most engineering concern, however, arises not from whether the geometrical spreading is $1/R^{1.3}$ or $1/R$ at close distances, but from whether a region of flat or increasing geometrical spreading at intermediate distances is present, as long as $\Delta\sigma$ is constrained by data that are largely at distances of 100 km–800 km. The simple $1/R$ model fits the sparse data for the eight events as well as do more complex models determined from larger datasets (where the larger datasets were used in our previous ground-motion prediction equations); this suggests that uncertainty in attenuation rates is an important component of epistemic uncertainty in ground-motion modeling. For the attenuation model used by Atkinson and Boore (2006), the average value of $\Delta\sigma$ from the point-source model ranges from 180 bars to 250 bars, depending on whether or not the stress parameter from the 1988 Saguenay earthquake is included in the average. We also find that $\Delta\sigma$ for a given earthquake is sensitive to its moment magnitude **M**, with a change of 0.1 magnitude units producing a factor of 1.3 change in the derived $\Delta\sigma$.

Introduction

The relative lack of ground-motion recordings from moderate-to-large earthquakes in eastern North America (ENA) necessitates the use of simulated ground motions for the development of ground-motion prediction equations and for engineering design for ENA. Fundamental to these simulations is a description of the source spectral scaling, by which is meant the magnitude dependence of the shape and amplitude of the spectrum. A number of source scaling models have been used in predictions of ground motions in ENA (e.g., Atkinson and Boore, 1998). Recently, Atkinson and Boore (2006) published ground-motion prediction equations for ENA based on finite-fault simulations using the program EXSIM. The stress parameter ($\Delta\sigma$) in the simulations used by Atkinson and Boore (2006) was 140 bars, based primarily on fitting short-period (0.2 sec and 0.1 sec) response spectra data from eight well-recorded earthquakes in ENA with EXSIM simulations (though other data were also considered, including inferred stress parameters from historical earthquakes).

The purpose of this article is to reexamine the value of the stress parameter for the eight well-recorded ENA earthquakes considered by Atkinson and Boore (2006). There are several motivations for doing that: (1) it would be convenient for a number of purposes (e.g., the development of the hybrid empirical ground-motion prediction equations of Campbell, 2003) if a point-source simulation program (such as SMSIM; Boore, 2003, 2005) could be used to generate ground motions rather than a finite-fault simulation program as used by Atkinson and Boore (2006); (2) recent work shows that there are systematic differences in motions from the original EXSIM (used by Atkinson and Boore, 2006) and a revised version of EXSIM, and thus a different value of stress parameter should be used for ENA with the revised EXSIM (Atkinson et al., 2009; Boore, 2009); (3) there have been some changes in the database parameters (distances, magnitudes, and spectral values) used by Atkinson and Boore (2006) in determining $\Delta\sigma$; and (4) these eight events are sufficiently important to ENA ground-motion prediction to warrant individual modeling and evaluation.

Due to trade-offs between source and attenuation parameters, an important component of the determination of source parameters is an examination of their sensitivity to uncertainty in the adopted attenuation model. We have addressed this uncertainty by considering four attenuation models in this article: the attenuation model of Atkinson (2004), as

adopted by Atkinson and Boore (2006), and three other alternative models. Two of the alternative attenuation models were used in our earlier studies and differ fundamentally from the model used by Atkinson and Boore (2006) in having a geometrical spreading that goes as $1/R$ rather than $1/R^{1.3}$ for distances less than 70 km (the $1/R^{1.3}$ attenuation model is from Atkinson, 2004). The third alternative model is specified by $1/R$ geometrical spreading at all distances. These alternative models are included to illustrate the sensitivity of the stress parameter to the attenuation model and to explore the consequences for near-source predictions of motion when the stress parameter is determined from fitting observations that are primarily at greater distances. The attenuation models considered in this article span a wide range of possible models and thus give some insight into how uncertainty in the attenuation model affects the stress parameter and near-source ground motions.

Data

Information regarding the earthquakes considered in this article is given in Table 1. The 2005 Riviere du Loup earthquake was particularly well recorded, and the Geological Survey of Canada has recently released many strong-motion recordings at distances within 200 km; these data were not available to Atkinson and Boore (2006), but they have been incorporated into our analysis.

The pseudo-absolute response spectral accelerations (PSA, the maximum response of a 5% damped single-degree-of-freedom oscillator as a function of vibration period) used by Atkinson and Boore (2006) are in their electronic supplement (see the Data and Resources section). We compared these values to the following motions when available: (1) PSA computed from time series provided by Linda Seekins (personal commun., 2009); and (2) PSA values from the Engineering Seismology Toolbox (see the Data and Resources section). Direct comparisons showed that the PSA from all three sources were usually in good agreement. When differences occurred, we generally used PSA from sources (1) or (2), as the instrument corrections and processing procedures are judged to be more consistent and accurate than those available to Atkinson and Boore (2006). We also plotted the PSA for a given period versus distance to look for outliers, and eliminated records from a few stations on this basis, under the

assumption that a significant outlier (based on subjective judgment, but generally differing from the median by more than a factor of about 10) is most likely to reflect a data error. Some records from broadband velocity sensor stations were also deleted because the instruments were clearly overdriven. Some details concerning the record processing are contained in Atkinson (2004). The corner frequencies of the high- and low-pass filters used in the processing are well outside of the frequency passband of most concern to us (5 Hz to 10 Hz) and do not affect the PSA values used to derive the stress parameters.

We evaluated the moment magnitude and distances used in Atkinson and Boore (2006), and this resulted in a few important changes. First, the distances for the 23 December 1985 Nahanni earthquake are based on the PEER NGA fault model (B. Chiou, personal commun., 2009), which uses a larger rupture surface than in Atkinson and Boore (2006); thus, the distances to the stations are generally smaller (the distances used in the simulations here are R_{EFF}, which accounts for fault finiteness when used in point-source simulations, as discussed by Boore, 2009; for the other events, the fault dimensions are much smaller than the fault-to-station distances, and therefore the hypocentral distances were used as a surrogate for R_{EFF}). Second, we use a different moment magnitude for the 6 March 2005 Riviere du Loup earthquake. As shown in Table 1, the value of 5.0 used in Atkinson and Boore (2006) has been changed to 4.7 based on waveform modeling by Won-Young Kim of Lamont-Doherty Earth Observatory (see the Data and Resources section). As we will show later, this change in magnitude results in a factor of 2.6 increase in the derived stress parameter for this event.

Our intent is to use data only from hard-rock stations. While a systematic evaluation of the site conditions at each recording station is beyond the scope of this article, we have eliminated obvious soil stations, such as a number of those in southern Ontario.

Following Atkinson and Boore (2006), our analysis used horizontal-component data where available; if horizontal-component data were not available, we converted observed vertical-component PSA to equivalent horizontal-component PSA by using the horizontal/vertical factors in the supplement to Atkinson and Boore (2006), which are based on Siddiqqi and Atkinson (2002).

Table 1
Event Information and $\Delta\sigma$, from Atkinson and Boore (2006)

Date (yyyy-mm-dd)	Name	Depth (km)	**M** (this article)	**M** (Atkinson and Boore, 2006)	$\Delta\sigma$ (Atkinson and Boore, 2006)
1985-12-23	Nahanni	8	6.8	6.8	134
1988-11-25	Saguenay	29	5.8	5.8	500
1990-10-19	Mount Laurier	13	4.7	4.7	250
1997-11-06	Cap Rouge	22	4.4	4.5	104
1999-03-16	St. Anne des Monts	19	4.5	4.5	85
2000-01-01	Kipawa	13	4.7	4.7	105
2002-04-20	Ausable Forks	11	5.0	5.0	149
2005-03-06	Riviere du Loup	13	4.7	5.0	125

The magnitude-distance distribution of our data is shown in Figure 1. Clearly, there is little constraint on the motions at distances of most engineering concern (within about 100 km); the bulk of the data are at distances greater than 100 km, and it is those data that will constrain the stress parameter. For this reason, simulations using different attenuation models can provide equally good fits to the bulk of the data, but imply very different motions at distances of engineering interest, as shown later.

Procedure for Estimating the Stress Parameter

As in Atkinson and Boore (2006), the stress parameter for each earthquake was determined from short-period PSA (0.2 sec and 0.1 sec) within 800 km. We use PSA rather than Fourier acceleration spectra, even though this involves a modeling assumption about the duration of motion with distance, for two reasons: (1) the electronic supplement to Atkinson and Boore (2006), which forms the core of our database, only provides PSA; and (2) we ultimately are interested in a model that predicts PSA for engineering purposes.

We used the stochastic point-source simulation program tmrs_rv_drvr, one of the SMSIM programs (Boore, 2005), for the simulations (using R_{EFF} for the Nahanni earthquake and hypocentral distance for the other events, whose fault rupture dimensions were small compared with the hypocentral distances). For a given earthquake and oscillator period, motions were simulated at the distance of each recording for a suite of stress parameters ($\Delta\sigma$), ranging from 6.25 bars to 3200 bars, incremented by a factor of 2. A residual, defined as $\log(PSA_{OBS}/PSA_{SIM})$, was computed for each observation for a given stress parameter. The arithmetic average of all residuals for rock stations within 800 km that recorded the
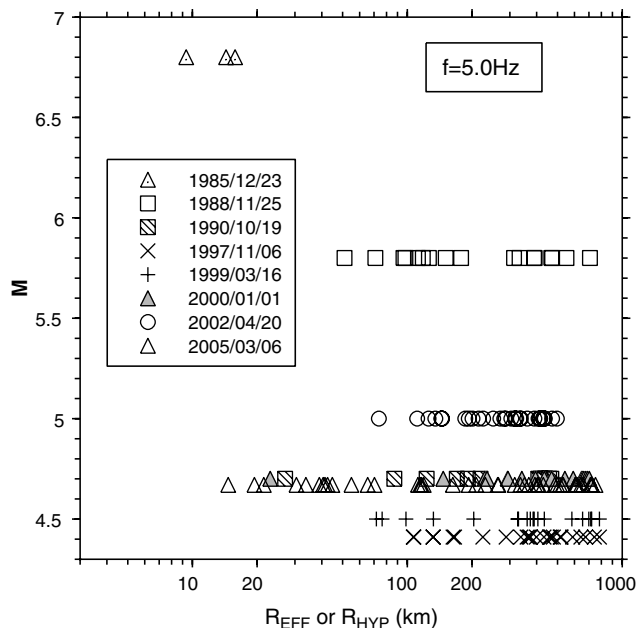
earthquake was computed, treating each observation as an independent variable. Plots of the average residual against $\log \Delta\sigma$ showed that in most cases a straight line provided a good fit to the data, but in a few cases a quadratic provided a better fit. In order to find the best value of $\Delta\sigma$ for a given earthquake and a given oscillator period, we fit a quadratic to the average residual, $\log \Delta\sigma$ pairs of values, and solved for the value of $\log \Delta\sigma$ that gave zero residual.

We computed four sets of simulations, one set for each attenuation model. The common parameters for each attenuation model are given in Tables 2, 3, and 4; these are the parameters used in Atkinson and Boore (2006). Note in particular that the same duration model is used for all attenuation models; this is so because the duration model, from Atkinson and Boore (1995) (hereafter AB95), is based on observations that are independent of the attenuation model. The attenuation models, divided into the geometrical spreading and the anelastic attenuation components, are given in Table 5. As shown in the table, the geometrical-spreading functions in the Atkinson (2004) model (hereafter A04) and the AB95 models are trilinear (in terms of log amplitude and log distance), whereas that in the Boore and Atkinson (1992) model (hereafter BA92) is bilinear, and the $1/R$ model is given by a single function of distance. A major difference in the A04 model and the other models is the rate of decay within 70 km: $1/R^{1.3}$ for A04 and $1/R$ for the others. We note that the $1/R^{1.3}$ rate of A04 is based on empirical regression of a large ENA database of Fourier spectra from small-to-moderate events (including many more events than those examined here); these data provide compelling evidence that the geometric spreading rate within 70 km is faster than $1/R$. Similar trends have been noted for small-to-moderate events in other regions (Allen et al., 2007; Atkinson and Morrison, 2009), but have not been confirmed for large events. Another important difference in the models is whether they contain a transition zone of no or slightly increasing geometrical spreading for distances spanning 100 km, that accommodates a Moho bounce effect: the A04 and the AB95 models contain such a transition zone; the BA92 and $1/R$ models do not. Finally, all models but the $1/R$ model feature geometrical spreading of $1/\sqrt{R}$ at distances beyond 100 km to 140 km (with the transition distance depending on the model).

Figure 1.   Magnitude and distance distribution of data used in this article.

Table 2

Key Parameters Used in Simulations (Excluding the Attenuation Model), from Atkinson and Boore (2006)*

Parameter	Value
Source model	Single-corner-frequency ω^{-2}
Partition factor	0.71
Average radiation pattern	0.55
Free-surface effect	2.0
Shear-wave velocity (at source depth) (β)	3.7 km/sec
Density (at source depth) (ρ)	2.8 gm/cm^3
Kappa (κ)	0.005 sec

*See Boore (2005) for use of parameters.

Table 3

Distance Dependence of Duration Used in the Simulations, from Atkinson and Boore (2006)*

Distance (km)	Duration (sec)
≤ 10.0	0.0
70.0	9.6
≥ 130.0	$7.8 + 0.04(R - 130)$

*The durations for nontabulated distances are determined by interpolation of the tabulated values (Boore, 2005).

Table 4

Crustal and Site Amplification Used in Simulations, from Atkinson and Boore (2006)*

Frequency (Hz)	Amplification
≤ 0.5	1.00
1.0	1.13
2.0	1.22
5.0	1.36
≥ 10.0	1.41

*The amplifications for nontabulated frequencies are determined by interpolation of the tabulated values (Boore, 2005).

The simple $1/R$ model at all distances was motivated by the observation that the other attenuation models (in particular, the A04 and the AB95 models) resulted in an underestimation of motions at closer distances for several of the events (as shown in the figures in this article; the effect is most notable for the 2005 Riviere du Loup earthquake). We emphasize that this model is introduced for comparison purposes; at this time we are not proposing it as a new attenuation model (such a model was earlier proposed by Atkinson, 1989, but is generally considered simplistic based on larger datasets). The associated anelastic attenuation for the $1/R$ model was determined subjectively to provide overall attenuation equivalent to that from the A04 model for distances from 140 to 800 km (the combined attenuation for the A04 model was well-determined in this distance range, and as shown in Figure 2, it is very similar to that found by Benz *et al.*, 1997). Figure 2 shows the comparison between the combined geometrical-spreading Q attenuation function for the A04 and the $1/R$ models used in this article. Given the usual scatter in ground-motion observations, it would be difficult to differentiate between these models with data spanning a limited distance range. Fitting the PSA at periods of 0.2 and 0.1 sec separately results in somewhat different values of Q (2700 and 3000), which can be accommodated by a function of Q that decreases with frequency. This functional dependence is counter to the observed frequency dependence of Q from many studies, at least at high frequencies. Because the two values of Q are close to one another, we used a constant-Q model, with Q given by the geometric mean (2850) of the 0.2 sec and 0.1 sec Q values.

Results

The derived stress parameters, based on the stochastic point-source modeling, are given for each of the four attenuation models in Table 6. It is important to note from the table that the $\Delta\sigma$ implied by the motions for the two modeled oscillator periods are close to one another, indicating consistency between the data and the model being used to simulate the data. Geometric means of the stress parameters in Table 6 for each attenuation model are given in Table 7, where the means have been computed with and without the stress parameters from the Saguenay earthquake. We singled out the Saguenay earthquake because its stress parameter is so much higher than those from the other earthquakes (see, e.g., Boore and Atkinson, 1992). A much-debated question is whether the stress parameter for the Saguenay earthquake represents a sample from a log-normal distribution of stress parameters or whether it is an outlier; the answer to this question (which is beyond the scope of this article) is important for calculations of interevent uncertainty and thus probabilistic seismic hazard analysis, particularly at low annual frequencies of exceedance. We simply present the average stress parameter with and without the Saguenay earthquake, noting that the use of a geometric mean decreases the sensitivity of the average stress parameter to the high values for the Saguenay earthquake.

Table 5

Attenuation Model Parameters*

Model	Reference	B	R_{min}(km)	Q	β (km/sec)
A04	Atkinson (2004)	-1.3	0	$\max(1000, 893f^{0.32})$	3.7
		$+0.2$	70	–	–
		-0.5	140	–	–
AB95	Atkinson and Boore (1995)	-1.0	0	$680f^{0.36}$	3.8
		$+0.0$	70	–	–
		-0.5	130	–	–
BA92	Boore and Atkinson (1992)	-1.0	0	$695f^{0.52}$	3.8
		-0.5	100	–	–
$1/R$	–	-1.0	0	2850	3.7

*The geometric spreading function is piecewise continuous, with the distance dependence in each segment given by R^b, where the function applies from R_{min} given for a particular value of b to R_{min} for the next value of b in the table for the same model. The anelastic function is $\exp(-\pi fR/Q\beta)$.
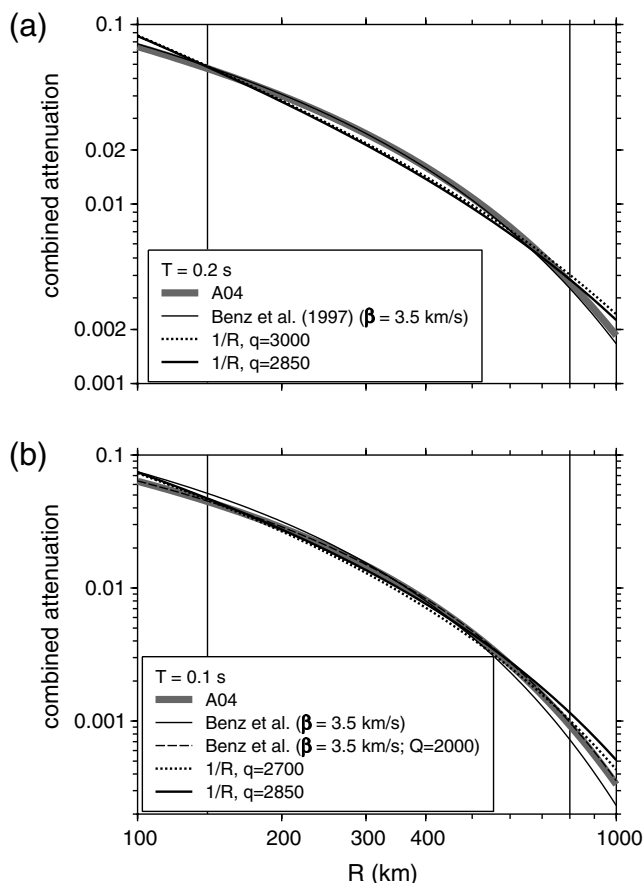
Figure 2. Equivalence in the overall attenuation between A04 and the $1/R$, Q combination given in the legend, for two values of period. The combined attenuation curves from Benz et al. (1997) for the northeastern United States and southeastern Canada (see text) are shown for comparison. All curves were adjusted vertically to give a subjective overall fit to the A04 curves between 140 and 800 km (these distances are shown by the vertical lines). Q was adjusted to give a reasonable subjective agreement for this same distance range. The results are shown for Q's chosen for each period independently, and for a constant Q (the geometric mean of the two independently chosen Q's). Distances < 100 km are not shown.

A comparison of the observed and predicted PSA for the three sites that recorded the Nahanni earthquake is shown in Figure 3. Two versions of the observed PSA at Nahanni station

1 are shown, one computed from the whole record and one from the portion of the record before the large acceleration peaks occurring late in the record (Weichert et al., 1986). We think that the large acceleration peaks are difficult to explain physically, although Weichert et al. (1986) offered an explanation in terms of relative locations of subevents on the main rupture surface. Although we used the PSA from the whole record in determining $\Delta\sigma$, we show the alternate PSA values for those who would like to see the effect of the large acceleration peaks on the response spectra at all periods.

Unlike the Nahanni earthquake, the data for the remaining seven earthquakes are for a wide range of distances, and thus the comparisons between observed and simulated data are in the form of plots of PSA versus distance. These comparisons are shown in Figures 4 through 10. Each figure also includes a map of the stations that provided data used to determine $\Delta\sigma$. Following Atkinson and Boore (2006), only data within 800 km were used in the determination of the stress parameters, although the upper graph in each figure shows data beyond this distance. Because the figures for both the 0.2 sec and 0.1 sec PSA are similar, we only show results for the 0.2 sec PSA.

The 2005 Riviere du Loup earthquake was particularly well recorded; as a result, we include in Figure 11 graphs of the 1 sec and 2 sec spectral amplitudes versus distance, along with the simulations using the geometric mean of $\Delta\sigma$ determined from the 0.2 sec and 0.1 sec PSA. These graphs show that the models based on the shorter period data do a reasonable job of predicting the longer period data. We also show in Figure 11 the importance of moment magnitude on the stress parameter estimates, as discussed in the next section. This is done by plotting the Atkinson and Boore (2006) predictions (which were based on a stress parameter of 140 bars with the original EXSIM model) for the originally assigned **M** 5.0, in addition to the revised value of **M** 4.67. The long-period PSA values at closer distances are more consistent with the larger moment estimate. Furthermore, a given stress parameter (140 bars for Atkinson and Boore, 2006) implies larger amplitudes at short periods if the associated moment is larger.

Table 6
$\Delta\sigma$ for Individual Events from Fitting PSA at Two Periods with SMSIM, for the Four Attenuation Models*

Date (yyyy-mm-dd)	**M**	A04		AB95		BA92		1/R	
		0.2 sec	0.1 sec	0.2 sec	0.1 sec	0.2 sec	0.1 sec	0.2 sec	0.1 sec
1985-12-23	6.8	155	137	58	52	57	51	56	51
1988-11-25	5.8	2161	2130	434	467	603	513	650	629
1990-10-19	4.7	317	304	59	73	81	69	108	108
1997-11-06	4.4	127	125	25	31	34	27	45	45
1999-03-16	4.5	107	108	23	28	28	23	38	38
2000-01-01	4.7	123	127	30	36	36	27	50	49
2002-04-20	5.0	183	168	40	42	57	43	76	68
2005-03-06	4.7	525	511	88	115	102	97	123	136

*The $\Delta\sigma$ values are in the columns below the oscillator periods, with units of bars.

Table 7
$\Delta\sigma$ Computed as the Geometric Mean of the Values
from Table 6, with and without Saguenay

Attenuation Model	$\Delta\sigma$ (include Saguenay)	$\Delta\sigma$ (exclude Saguenay)
A04	249	183
AB95	59	45
BA92	63	47
$1/R$	86	64

Uncertainty of $\Delta\sigma$

The standard deviation of the residual for each earthquake and each attenuation model is given in Table 8, for a 0.2 sec oscillator and for the optimum stress parameter for each attenuation model and each earthquake. The standard deviations were computed for the residuals, defined as log(PSA$_{OBS}$/PSA$_{SIM}$), but for convenience they are given as factors (residuals can be defined in terms of natural or common logarithms, but giving the multiplicative factor corresponding to the standard deviation removes any ambiguity as to which base was used). For reference, the intraevent standard deviation from recent ground-motion prediction equations corresponds to a factor of about 1.7 (Boore and Atkinson, 2008), which is comparable to the standard deviations reported for most of the earthquakes in Table 8. It is also worth noting that for a particular earthquake the standard deviations are generally similar for the four attenuation models, supporting the statement that the limited observations from these eight events are equally well fit by the four models.

The true value of the uncertainty of $\Delta\sigma$ is hard to quantify, because some of the components of the uncertainty are difficult to estimate. The easiest component to estimate is the error involved in solving for the value of $\Delta\sigma$ that gives zero average residual. There is little scatter in the plots of the average residual versus log $\Delta\sigma$, and thus there is little uncertainty in the optimum value of $\Delta\sigma$ for a given set of observations and simulation model; formal estimates of the error using propagation of errors generally correspond to factors much less than 1.1.
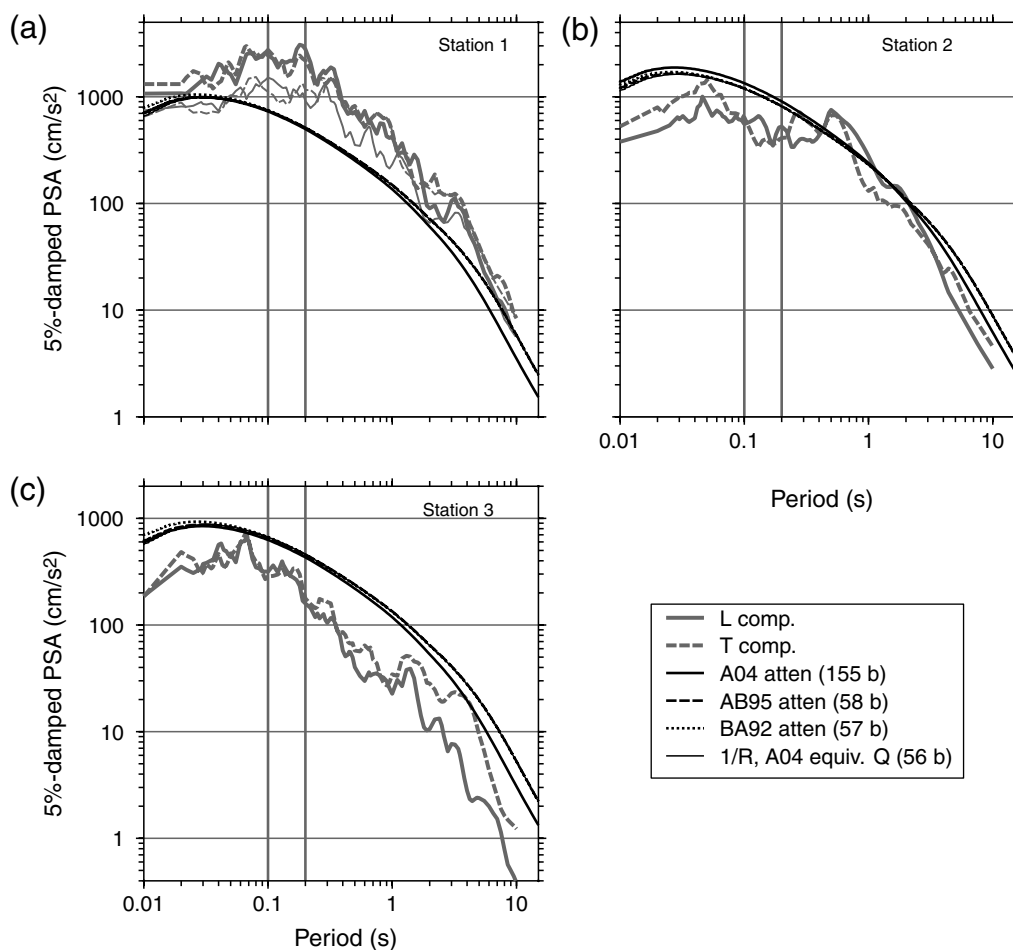

Figure 3. Observed and predicted response spectra for the 1985 Nahanni earthquakes at stations (a) 1, (b) 2, and (c) 3. The stress parameters (given in parenthesis) for the AB95, BA92, and $1/R$ attenuation models are so similar that the predicted spectra for these three models are almost indistinguishable (the simulations are for the stress parameters determined for a 0.2 sec oscillator; see Table 6). The heavy vertical lines show the periods from which $\Delta\sigma$ was determined. The thin gray lines in graph (a) show the PSA from the first 7.5 sec of the record.
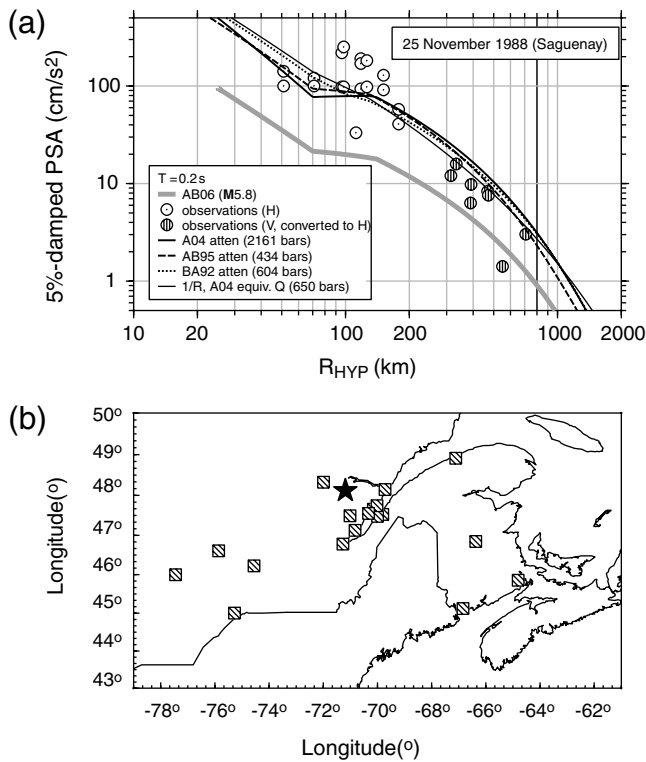
Figure 4. (a) Observations and predictions versus distance for the 1988 Saguenay earthquake; (b) the epicenter (star) and stations for which data were used to determine $\Delta\sigma$.

Figure 5. (a) Observations and predictions versus distance for the 1990 Mount Laurier earthquake; (b) the epicenter (star) and stations for which data were used to determine $\Delta\sigma$.

Another component of the error is the distribution of observations used to define the average residual. Except for the Nahanni earthquake, there seem to be enough observations to provide a good estimate of the stress parameter, assuming that a particular attenuation model is correct. The particularly well-recorded 2005 Riviere du Loup earthquake allows us to test this statement. We repeated the determination of $\Delta\sigma$ using various subsets of the 0.2 sec PSA data: (1) the Engineering Seismology Toolbox (ESTB) dataset used previously; (2) the ESTB dataset, plus data from two additional stations (LOZ at 515 km, and NCB at 549 km); (3) the vertical components for the ESTB dataset; (4) the horizontal components for the ESTB dataset; (5) the ESTB data for distances beyond 40 km; and (6) a subset of the ESTB dataset for stations not available before the recent (2010) release of the Geological Survey of Canada accelerometric data (what we call the pre-2010-stations were primarily from broadband velocity sensor transducers; for this last subset we used the more recent accelerometric data, but only at those stations for which the earlier velocity recordings were available). The values of $\Delta\sigma$ determined for these subsets of the data are given in Table 9. The distribution of the data used for these various subsets is shown in Figure 12, along with the simulated motions for the extreme values of $\Delta\sigma$, as well as for the whole ESTB dataset. It seems that just using horizontal data only or vertical data only makes little difference in the stress parameter. The biggest difference in $\Delta\sigma$ is the value obtained using the pre-2010-
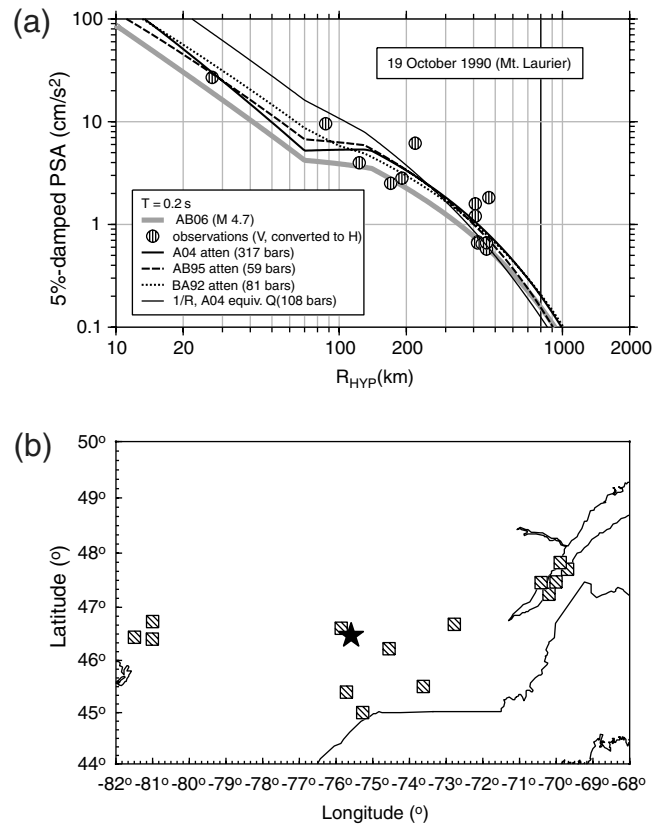
stations data, as compared with the values obtained using the more complete recent dataset, which not only has more data at distances less than 40 km or so, but also more data in the 100–200 km range. The lesson here is that the distribution of data with distance is an important factor in determining $\Delta\sigma$. The range of log $\Delta\sigma$ over the subsets is similar for the various attenuation models, corresponding to a factor of about 1.5, suggesting that the uncertainty in $\Delta\sigma$ for the older, less well-recorded earthquakes may be similar.

Another source of uncertainty in the determination of $\Delta\sigma$ is related to the sensitivity of the high-frequency spectral level to the moment magnitude. We were motivated to consider this source of uncertainty by the change in the moment magnitude of the Riviere du Loup earthquake from 5.0 used in Atkinson and Boore (2006) to 4.67 used in this article. Figure 13 shows the determined stress for the Riviere du Loup earthquake as a function of the assumed magnitude for the earthquake. Also shown is the theoretical dependence given by the requirement of a constant high-frequency level of the Fourier acceleration spectrum (FAS) for combinations of the stress parameter and the moment magnitude (the dependence is not the same as for PSA because of the effect of duration in PSA, as well as the fact that PSA at a given period is not necessarily simply related to the FAS at the same period). Clearly, the value of $\Delta\sigma$ is quite sensitive to the
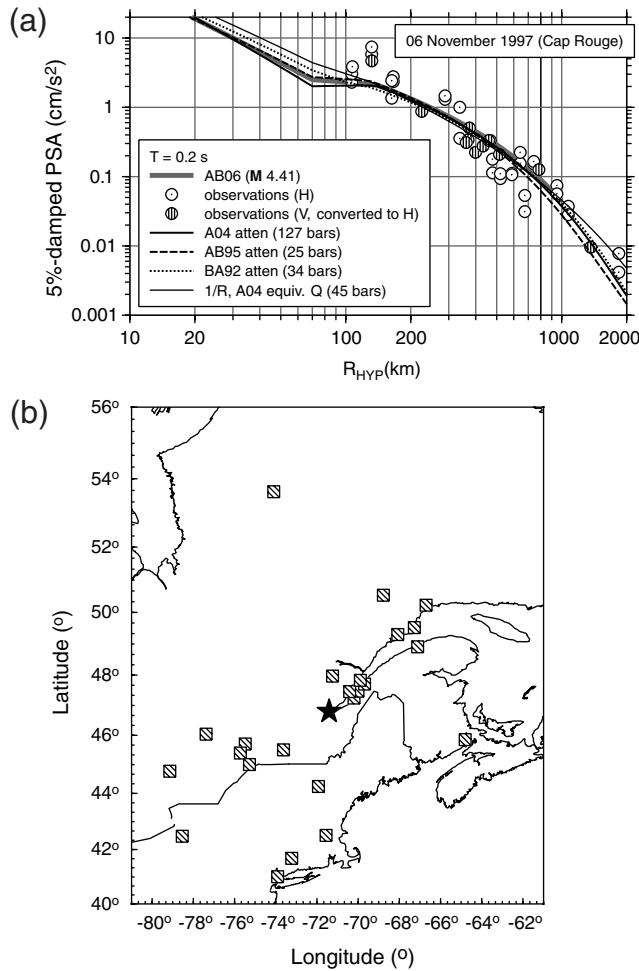
Figure 6. (a) Observations and predictions versus distance for the 1997 Cap Rouge earthquake; (b) the epicenter (star) and stations for which data were used to determine $\Delta\sigma$.

Figure 7. (a) Observations and predictions versus distance for the 1999 St. Anne des Monts earthquake; (b) the epicenter (star) and stations for which data were used to determine $\Delta\sigma$.

magnitude. Approximating the dependence by a linear trend gives the equation

$$\frac{\partial \log(\Delta\sigma)}{\partial \mathbf{M}} \approx -1.2 \qquad (1)$$

(we emphasize that this equation gives the relation between changes in $\Delta\sigma$ and $\mathbf{M}$ under the constraint that the high-frequency spectral level is fixed). As an example of what this equation implies, considering an uncertainty in $\mathbf{M}$ of 0.1 (this uncertainty is an estimate based on personal experience as well as an analysis of the statistical uncertainties in the Next Generation Attenuation flatfile of global strong-motion data, available from http://peer.berkeley.edu/nga/flatfile.htm, last accessed 23 February 2010), the uncertainty will generally be higher than this for older, small-magnitude earthquakes. Equation (2) states that this uncertainty will translate into an uncertainty of 0.12 in $\log \Delta\sigma$ (a factor of 1.3). This is a much more important source of uncertainty in $\Delta\sigma$ than the error involved in fitting the average residuals to the stress parameters. We conclude that the uncertainty in $\Delta\sigma$ for a
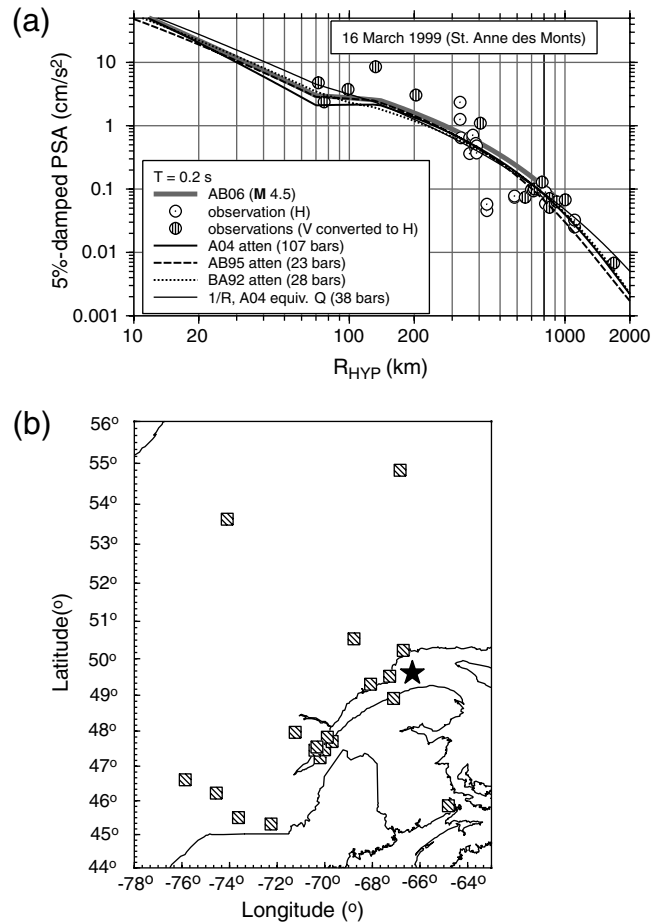
given attenuation model could be as much as a factor of 1.3 or more.

The most pervasive uncertainty in determination of the stress parameter is the choice of the correct attenuation model for the study events. All of the attenuation models give comparable fits to the observations used in this study, but the stress parameters are dependent on the attenuation models, as shown in the tables. In particular, the A04 model with $1/R^{1.3}$ decay within 70 km implies a much larger stress parameter than the other models, for which the decay is $1/R$ within at least 70 km. The reason for the large differences is clear: for a given attenuation model, the stress parameter is adjusted to fit the bulk of the data, most of which is beyond 100 km. Therefore, extrapolating the steeper $1/R^{1.3}$ decay back to the source gives a larger value of the source spectrum and thus a higher stress parameter. What may be surprising are the very similar stress parameters for the AB95 and the BA92 models; this is a consequence of the combined geometrical spreading and Q attenuation leading to similar ground-motion amplitudes in the distance range of most observations for the same value of $\Delta\sigma$, even though the simulated motions at closer distances are quite different.
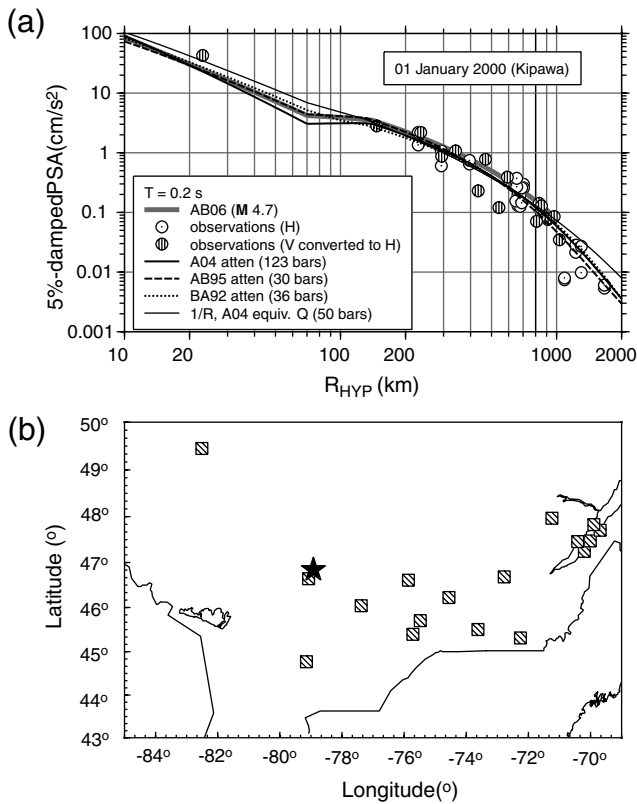
Figure 8. (a) Observations and predictions versus distance for the 2000 Kipawa earthquake; (b) the epicenter (star) and stations for which data were used to determine $\Delta\sigma$.

It is important to recognize that the value of stress parameter in this exercise is determined within the context of a fixed seismic moment, as based on independent estimates. In reality, each of the attenuation models will imply a different moment level of the response spectrum, in addition to a different high-frequency level. Some of the noted differences in stress parameters between attenuation models may thus be attributable to an overall bias in source level that affects the long-period end of the spectrum as well as the high-frequency end; such a bias may occur when extrapolating a particular attenuation model all the way back to the source. Specifically, earlier estimates of **M** 5.0 for the Riviere du Loup earthquake (from Atkinson and Boore, 2006) were based in part on extrapolating spectra back to the source using the A04 attenuation model. The near-source observations at longer periods for this earthquake are inconsistent with **M** 4.7, if an attenuation of $R^{-1.3}$ is assumed to continue all the way back to the source. This point can be appreciated in Figure 11, in which the Atkinson and Boore (2006) predictions for **M** 5.0 are also shown for comparison. If we assigned a moment magnitude that would fit the long-period PSA for each event under the given attenuation model (rather than using an independently determined fixed moment), we would infer different stress parameters. However, we would continue to reproduce the ground-motion observations at distance, provided internal consistency of the models were maintained (i.e., the same
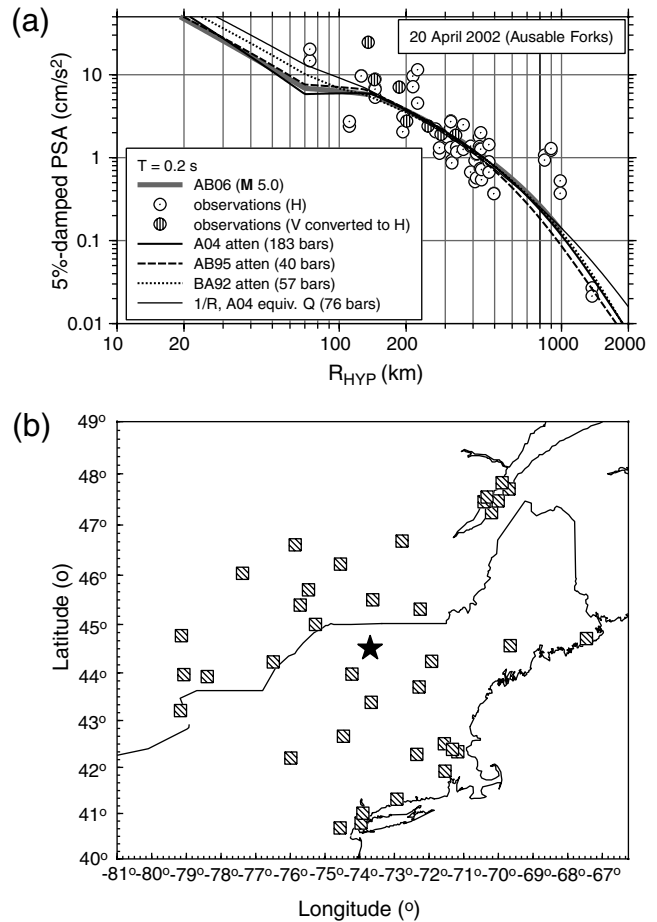

Figure 9. (a) Observations and predictions versus distance for the 2002 Ausable Forks earthquake; (b) the epicenter (star) and stations for which data were used to determine $\Delta\sigma$.

magnitude/stress drop combinations must be used in both backward and forward modeling).

Discussion

At distances less than about 100 km, there is a tendency for the models to underestimate the high-frequency ground-motion amplitudes, particularly for the Riviere du Loup earthquake (Fig. 10). This underestimation has been noted previously for a number of the earthquakes we used (C. Cramer, personal commun., 2005; Atkinson and Boore, 2006). It is important to understand that the A04 and the AB95 attenuation models were driven by larger datasets than those used in this article, including many smaller events. The tendency toward underestimation at close distances for the selected study events may be an artifact attributable to the sparse data, or alternatively, may reflect some bias in the small-magnitude attenuation models when applied to larger events.

We compare the new determinations of $\Delta\sigma$ for use with the point-source model with those from Atkinson and Boore (2006) (for use with the original EXSIM program) in Figure 14. For consistency with Atkinson and Boore (2006), the new $\Delta\sigma$ are for the A04 attenuation model. For several reasons
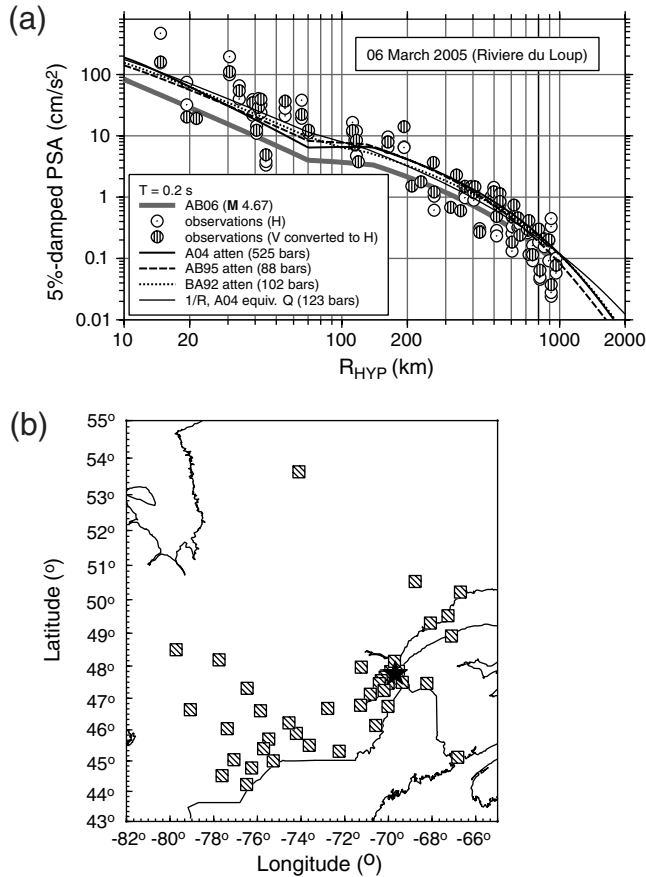
Figure 10. (a) Observations and predictions versus distance for the 2005 Riviere du Loup earthquake; (b) the epicenter (star) and stations for which data were used to determine $\Delta\sigma$.
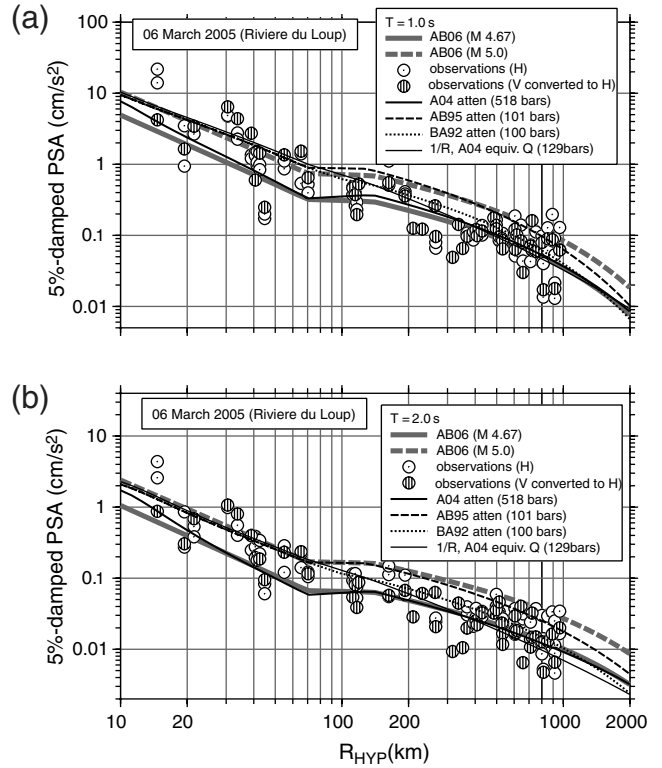

Figure 11. (a), (b) Observations and predictions versus distance for 1.0 sec and 2.0 sec PSA from the 2005 Riviere du Loup earthquake. The $\Delta\sigma$ values used in the simulations are given in parenthesis; they are the geometric means of the stress values determined for the 0.1 and 0.2 sec PSA data for each attenuation model. Heavy gray lines show Atkinson and Boore (2006) predictions for both the originally assigned **M** 5.0 for this event and for the revised value of **M** 4.67.

the estimates of $\Delta\sigma$ are larger than those reported in Atkinson and Boore (2006) for all events. The principal reason for the increase is the differences between SMSIM and EXSIM discussed in Atkinson *et al.* (2009) and Boore (2009); however, factors such as the data selection and the change in magnitude for two events also contribute to the increase. In addition, we point out that the Atkinson and Boore (2006) $\Delta\sigma$ value of 500 bars for the Saguenay earthquake was taken from Boore and Atkinson, 1992 (rather than being determined in Atkinson and Boore, 2006). Boore and Atkinson, 1992 assumed an attenuation model with $1/R$ geometrical spreading to 100 km; using the more rapid $1/R^{1.3}$ of A04 would have led to a considerably larger estimate of $\Delta\sigma$ (on the order of 2000 bars, as indicated in Table 6). As shown in Table 7, the geometric-average stress parameter from the point-source model ranges from 180 bars to 250 bars, depending on whether or not the stress parameter from the 1988 Saguenay earthquake is included in the average. We emphasize that this average stress parameter is applicable strictly to SMSIM point-source simulations (not to EXSIM as implemented in Atkinson and Boore, 2006).

Most of the observations used to determine the stress parameters are at distances of 100 km to 800 km, greater than

those of most engineering concern. To show better the similarities and differences in the ground-motion predictions at closer distances, in Figure 15 we replot the observed and predicted PSA for the 2002 Au Sable Forks earthquake (Fig. 9a), starting at 1 km. We chose the 2002 Au Sable Forks earthquake because it was relatively well recorded and because the stress parameter for a particular attenuation model

Table 8
Standard Deviation of Residuals Using Best-Fit Stress Parameters Determined Using Different Attenuation Models for 0.2 sec PSA*

Date (yyyy-mm-dd)	**M**	A04	AB95	BA92	$1/R$
1985-12-23	6.8	3.5	3.5	3.5	3.5
1988-11-25	5.8	2.0	1.8	2.0	1.8
1990-10-19	4.7	1.6	1.6	1.6	1.6
1997-11-06	4.4	1.9	1.8	1.9	1.8
1999-03-16	4.5	2.3	2.2	2.3	2.2
2000-01-01	4.7	1.5	1.6	1.5	1.5
2002-04-20	5.0	1.8	1.7	1.7	1.7
2005-03-06	4.7	2.2	2.1	2.1	2.0

*The standard deviations are expressed as multiplicative factors, although the standard deviations were computed for $\log(PSA_{OBS}/PSA_{SIM})$.

Table 9
$\Delta\sigma$ for 2005 Riviere du Loup Event from Fitting
0.2 sec PSA with SMSIM, for the Four
Attenuation Models*

Subset	A04	AB95	BA92	1/R
ESTB[†]	525	88	102	123
ESTB plus LOZ, NCB	515	87	101	122
ESTB: H only	541	89	101	117
ESTB: V only	506	87	105	131
ESTB: $R >= 40$ km	462	79	95	119
Subset of stations available before 2010	347	64	72	92

*$\Delta\sigma$ has units of bars.
[†]ESTB: Engineering Seismology Toolbox.

for that event is close to the median stress parameter over all events for that attenuation model. Before discussing the various curves, we note the distinctive kinks at 10, 70, and 130 km in the curve corresponding to the simple $1/R$ attenuation model. This is not an error, but is a consequence of the trilinear duration function (see Table 2) used in simulating the PSA; plots of FAS versus distance for the $1/R$ model would be smoothly varying. For this earthquake, the Atkinson and Boore (2006) equation and the two models with a flat or increasing geometrical spreading (the AB95 and A04 models) predict similar motions beyond about 20 km, in spite of the very different stress parameters; the differences in these models are only pronounced at distances closer than about 20 km because the stress parameters adjust the curves to be similar for distances for which observations are available. Recalling that the distance in the simulations is intended to be an effective distance to the rupture surface, the
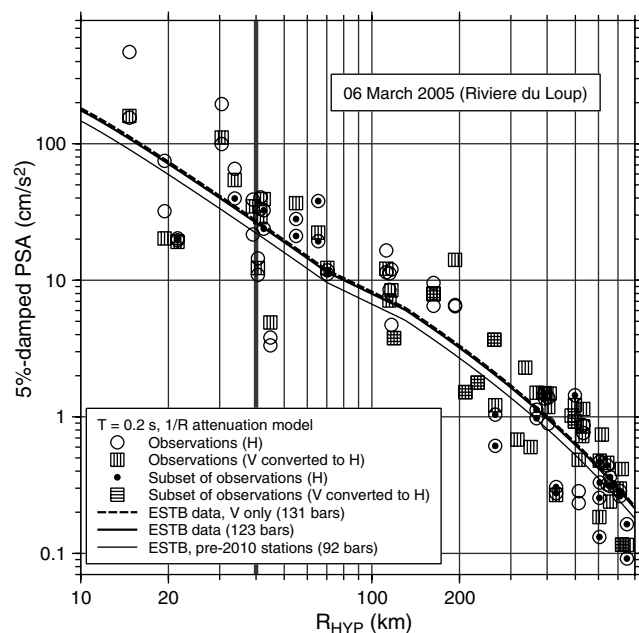
consequences of the differences in the motions within 10 km for hazard calculations may not be large (typical focal depths are near 10 km). The most important factor for ground motions at distances less than about 100 km is whether the attenuation models have a geometrical spreading that is flat or increasing in a distance range from 70 to about 130 km (a transition zone); such models predict lower ground motions than the simple $1/R$ model, with the two-part geometrical-spreading model of BA92 predicting ground motions between the two extremes. The presence of a transition zone in the attenuation behavior is supported by seismographic data from small earthquakes in ENA (Atkinson and Mereu, 1992; Atkinson, 2004), especially at frequencies near 1 Hz; this observational trend is usually interpreted as being due to critical angle reflections from within the crust or from the base of the crust (Burger *et al.*, 1987). It is interesting that the Moho bounce effect is very important for the interpretation of source parameters as deduced from regional ground-motion observations. It is possible that at high frequencies, and perhaps for larger earthquakes, there is no longer the constructive interference that produces the pronounced change in the geometrical spreading seen in lower-frequency data from smaller earthquakes. If so, the effective geometrical-spreading function may be frequency dependent, which would be difficult to accommodate in the existing stochastic-based simulation methods. Furthermore, confirmation of
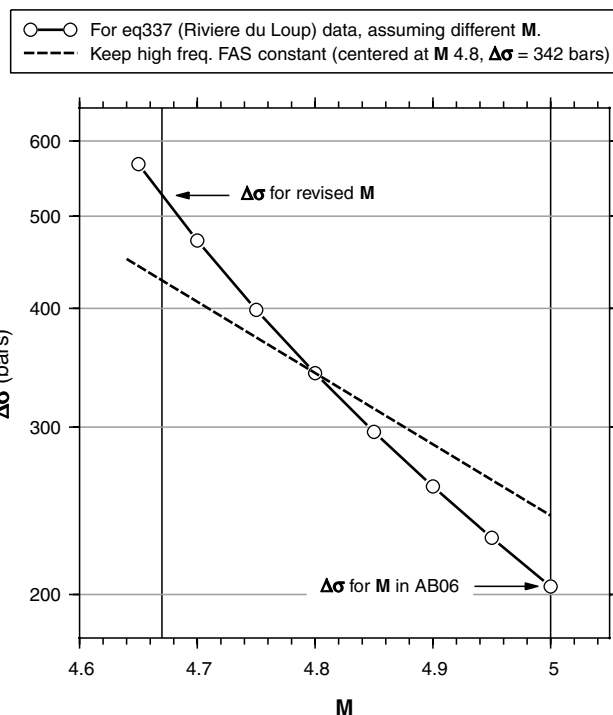

Figure 12. Different subsets of the data and the simulated results for three subsets of the ESTB data (see text).

Figure 13. Stress parameter as a function of assumed magnitude for the Riviere du Loup earthquake, using the A04 attenuation model. Note that the magnitude used in the calculations for this earthquake was 4.67 (as derived from the seismic moment of 1.15e23 dyne-cm [W.Y. Kim, written commun. to J. Boatwright, 2009]); this magnitude has been rounded to 4.7 in the tables.
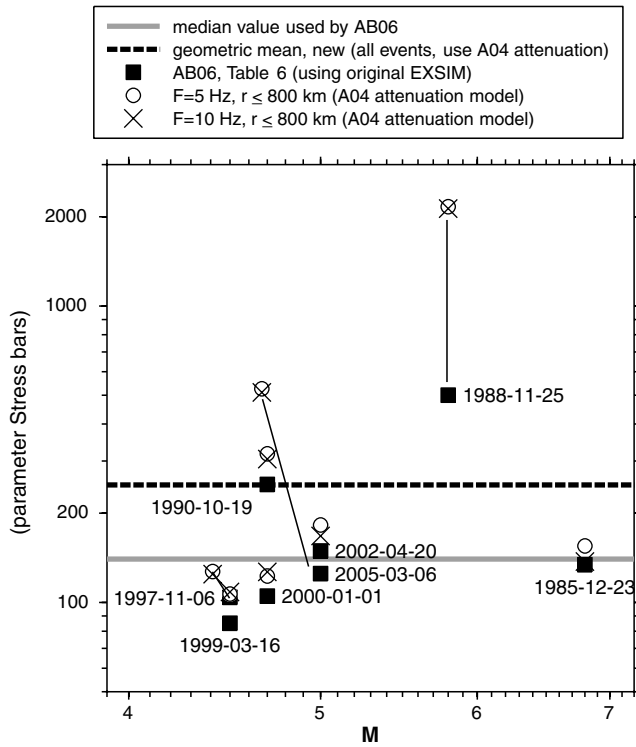
Figure 14. Summary of stress parameters. For two earthquakes (6 November 1997 [1997-11-06] and 6 March 2005 [2005-03-06]) the magnitude used in Atkinson and Boore (2006) and that used here differed; lines connect old and new stress parameters for these events (and also for the 25 November 1988 [1988-11-25] event, where there is a very large difference in stress parameters).
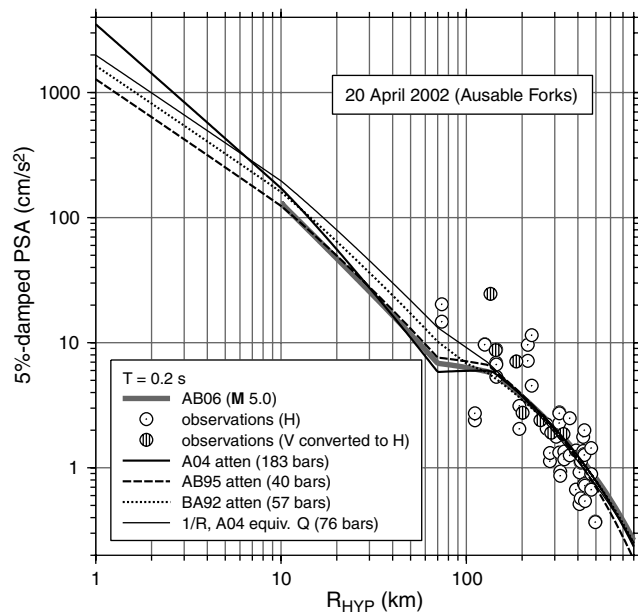
such a model must await richer ENA datasets from moderate-to-large magnitude earthquakes.

Figure 16 shows a comparison of the PSA predictions using the point-source stochastic model (SMSIM) with those from Atkinson and Boore (2006), which used the original EXSIM finite-fault stochastic model and a stress parameter of 140 bars, for magnitudes of 4.5, 5.5, and 6.5. For the point-source simulations we used three values of the stress parameter: 140 bars, 200 bars, and 250 bars. The point-source simulations used the SMSIM program tmrs_ff_rv_drvr, which calculates the effective distance for a finite-fault model. The top edge of the rupture surface for each earthquake is at 5 km (similar results are obtained for one with the top edge at 0.5 km), and the fault plane has a 50° dip. The rupture size was given by the Wells and Coppersmith (1994) equations for reverse faults, with changes in the rupture size being made to account for differences in the given stress parameter and an average of 70 bars that is assumed to be representative of the earthquakes in the Wells and Coppersmith database (e.g., Boore *et al.*, 1992). The motions were simulated along lines radiating at azimuths of 0°, 45°, and 90° from the center of the top edge of the fault. It is clear from Figure 16 that the effective point-source simulations using a constant stress parameter cannot be made to agree with the Atkinson and Boore (2006) motions for all magnitudes, even at large distances from the fault. For example, at distances beyond about 140 km the agreement is good for 140 bars for **M** 4.5, 200–250 bars

Figure 15. Observed and simulated PSA versus distance for the Ausable Forks earthquake, starting at 1 km to emphasize the difference in predicted ground motions at close distances.
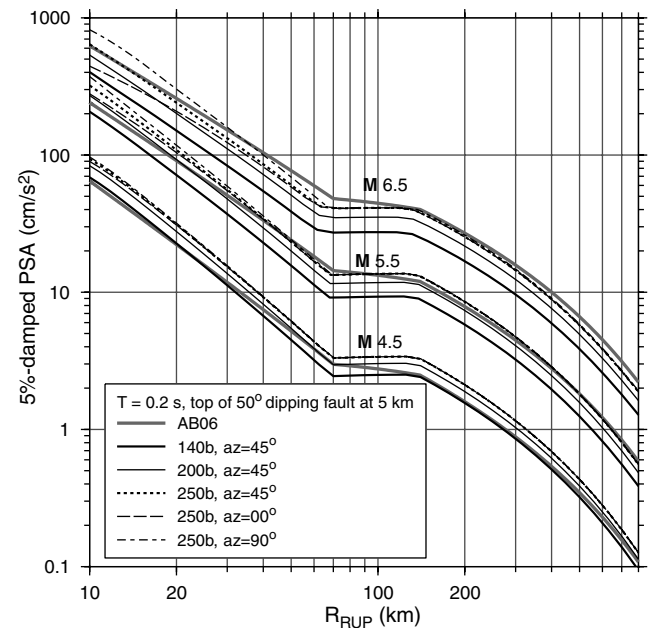

Figure 16. Comparison of PSA from Atkinson and Boore (2006) and SMSIM simulations using stress parameters of 140, 200, and 250 bars. The SMSIM calculations use effective distance computed for finite faults. The results for motions along lines at azimuths of 0°, 45°, and 90° from the midpoint of the fault are shown for the 250 bar stress parameter. The simulations are for magnitudes of 4.5, 5.5, and 6.5.

for **M** 5.5, and 250 bars for **M** 6.5. This disagreement was recognized by Boore (2009), who showed that although the Fourier acceleration spectra from both methods could be very similar, the shorter duration assumed by EXSIM leads to larger response spectral amplitudes (see fig. 8 in Boore, 2009). The effect is particularly important for shorter periods and larger magnitudes for which the source component of the overall duration is relatively more important than the path component, as compared with smaller magnitude earthquakes. We are not making a judgment here as to which are the best motions, but only show the comparison to alert readers to the differences that arise due to different simulation methods and assumptions. These differences might be considered as a significant source of epistemic uncertainty in ground-motion prediction equations derived from simulations.

Conclusions

We determined the stress parameters ($\Delta\sigma$) of eight well-recorded earthquakes in eastern North America. The new values of stress are applicable to the revised point-source stochastic method (Boore, 2009). We used four attenuation models: the A04 model with $1/R^{1.3}$ and $1/\sqrt{R}$ geometrical spreading at distances less than 70 km and greater than 140 km, respectively; the AB95 model with $1/R$ and $1/\sqrt{R}$ geometrical spreading at distances less than 70 km and greater than 130 km, respectively; the BA92 model with $1/R$ and $1/\sqrt{R}$ geometrical spreading at distances less than and greater than 100 km, respectively; and a model with geometrical spreading of $1/R$ at all distances. Each model gave similar fits to the bulk of the data from the study events, most of it being in the 100–800 km distance range. Estimates of $\Delta\sigma$ are particularly sensitive to the geometrical spreading within 70 km, with the implied stress parameter for the $1/R^{1.3}$ model of A04 being much higher than those from the other three considered attenuation models, all of which have $1/R$ spreading within the first 70 km. Obviously, the stress parameter and the attenuation model are closely linked together; the value of the stress parameter by itself cannot be meaningfully compared with other stress parameters determined using different attenuation functions (this is reminiscent of the close tie between geometrical spreading and Q). The A04 attenuation model gives a geometric-mean $\Delta\sigma$ ranging from 180 bars to 250 bars (as computed without and with $\Delta\sigma$ from the 1988 Saguenay earthquake), compared with the value of 140 bars used in Atkinson and Boore (2006). We emphasize that the new values of $\Delta\sigma$ are applicable to the point-source model used here (SMSIM) and does not apply to the original EXSIM algorithm used in Atkinson and Boore (2006).

Somewhat surprisingly, the most important difference in predicted ground motions at distances of most engineering concern arises not from the stress parameters determined in our study, but from whether the geometrical spreading includes a Moho bounce effect that causes a flat or increasing trend in motions over an intermediate range of distances (70 to about 130 km), as is the case for the AB95 and A04 attenua-

tions models. The simulated ground motions from these models are significantly lower than those from the BA92 and the $1/R$ attenuation models at distances from about 10 km to 130 km. This is a consequence of the stress being adjusted so that any given attenuation curve is pinned by the observations at distances primarily greater than 200 km. On the other hand, if the bulk of the data had been at distances within 200 km, it is likely that the predicted motions would be similar at close distances but different at larger distances. Thus, the shape of the attenuation curve over all distances is important if we wish to deduce source parameters from regional ground-motion observations.

A geometrical spreading of $1/R$ provides a satisfactory fit to the data from these events at all distances and is presented to show the sensitivity of the stress parameter and the ground-motion estimations to the attenuation model. The representative value of $\Delta\sigma$ for the simple $1/R$ model is close to 70 bars. We emphasize that the bulk of the data used to constrain the stress parameters are at distances greater than 100 km. This highlights the importance and potential pitfalls of the attenuation shape in using distant observations to determine source parameters with sparse data. We note that the A04 three-part attenuation model was based on more abundant data than that considered here; however, the data used by A04 are dominated by earthquakes of small magnitude (**M** < 5). Furthermore, the A04 geometric spreading model is assumed to be independent of frequency (with only the Q model depending on frequency), and it is possible that this is an oversimplification. Given that most of the earthquakes we modeled in this study are moderate in size, we would expect that the geometrical spreading should be similar to that from small earthquakes (i.e., point sources), and thus the A04 model should apply. However, the apparent ability of a simpler $1/R$ attenuation model at all distances to adequately model attenuation, and perhaps do a more robust job of inferring source parameters from sparse data, is noteworthy and warrants further investigation.

This article underscores the need for more data to verify geometrical-spreading rates over a wide range of distances, but most notably at distances less than about 200 km. In particular, we need to establish whether the attenuation models derived from the more abundant small-magnitude data are applicable to the modeling of attenuation from larger events and to determine if the geometrical-spreading function is frequency dependent.

Data and Resources

The response spectral values came from the electronic supplement of Atkinson and Boore (2006) (http://bssa .geoscienceworld.org/cgi/content/full/96/6/2181/DC1, last accessed 28 April 2010), the Engineering Seismology Toolbox (http://www.seismotoolbox.ca:80/, last accessed 28 April 2010), the Canadian Geological Survey (ftp:// ftp.seismo.nrcan.gc.ca/exports/adams/DraftRiviere-du-LoupSGMOpenFile/, last accessed 28 April 2010), and time

series provided by Linda Seekins of the U.S. Geological Survey. The moment magnitude of the 6 March 2005 Riviere du Loup earthquake is from a written communication from W.-Y. Kim to J. Boatwright in 2009; the moment magnitude of the 6 November 1997 Cap Rouge earthquake is from the seismic moment derived by R. Herrmann (http://eqinfo.eas.slu.edu/Earthquake_Center/MECH.NA/19971106023433/index.html, last accessed 28 April 2010).

The SMSIM programs used for the simulations can be obtained from the online software link on http://www.daveboore.com (last accessed 28 April 2010).

Acknowledgments

References

Allen, T., P. Cummins, T. Dhu, and J. Schneider (2007). Attenuation of ground-motion spectral amplitudes in southeastern Australia, *Bull. Seismol. Soc. Am.* **97,** 1279–1292.

Atkinson, G. M. (1989). Attenuation and site response for the eastern Canada telemetered network, *Seismol. Res. Lett.* **60,** 59–69.

Atkinson, G. M. (2004). Empirical attenuation of ground-motion spectral amplitudes in southeastern Canada and the northeastern United States, *Bull. Seismol. Soc. Am.* **94,** 1079–1095.

Atkinson, G. M., and D. M. Boore (1995). Ground motion relations for eastern North America, *Bull. Seismol. Soc. Am.* **85,** 17–30.

Atkinson, G. M., and D. M. Boore (1998). Evaluation of models for earthquake source spectra in eastern North America, *Bull. Seismol. Soc. Am.* **88,** 917–934.

Atkinson, G. M., and D. M. Boore (2006). Earthquake ground-motion prediction equations for eastern North America, *Bull. Seismol. Soc. Am.* **96,** 2181–2205.

Atkinson, G., and R. Mereu (1992). The shape of ground motion attenuation curves in southeastern Canada, *Bull. Seismol. Soc. Am.* **82,** 2014–2031.

Atkinson, G., and M. Morrison (2009). Regional variability in ground motion amplitudes along the west coast of North America, *Bull. Seismol. Soc. Am.* **99,** 2393–2409.

Atkinson, G. M., K. Assatourians, D. M. Boore, K. W. Campbell, and D. Motazedian (2009). A guide to differences between stochastic point-source and stochastic finite-fault simulation methods, *Bull. Seismol. Soc. Am.* **99,** 3192–3201.

Benz, H. M., A. Frankel, and D. M. Boore (1997). Regional *Lg* attenuation for the continental United States, *Bull. Seismol. Soc. Am.* **87,** 606–619.

Boore, D. M. (2003). Prediction of ground motion using the stochastic method, *Pure Appl. Geophys.* **160,** 635–676.

Boore, D. M. (2005). SMSIM—Fortran programs for simulating ground motions from earthquakes: Version 2.3—A revision of OFR 96-80-A, *U.S. Geol. Surv. Open-File Rept. 00-509*, revised 15 August 2005, 55 pp.

Boore, D. M. (2009). Comparing stochastic point-source and finite-source ground-motion simulations: SMSIM and EXSIM, *Bull. Seismol. Soc. Am.* **99,** 3202–3216.

Boore, D. M., and G. M. Atkinson (1992). Source spectra for the 1988 Saguenay, Quebec, earthquakes, *Bull. Seismol. Soc. Am.* **82,** 683–719.

Boore, D. M., and G. M. Atkinson (2008). Ground-motion prediction equations for the average horizontal component of PGA, PGV, and 5%-damped PSA at spectral periods between 0.01 s and 10.0 s, *Earthquake Spectra* **24,** 99–138.

Boore, D. M., W. B. Joyner, and L. Wennerberg (1992). Fitting the stochastic ω^{-2} source model to observed response spectra in western North America: Trade-offs between $\Delta\sigma$ and κ, *Bull. Seismol. Soc. Am.* **82,** 1956–1963.

Burger, R., P. Somerville, J. Barker, R. Herrmann, and D. Helmberger (1987). The effect of crustal structure on strong ground motion attenuation relations in eastern North America, *Bull. Seismol. Soc. Am.* **77,** 420–439.

Campbell, K. W. (2003). Prediction of strong ground motion using the hybrid empirical method and its use in the development of ground-motion (attenuation) relations in eastern North America, *Bull. Seismol. Soc. Am.* **93,** 1012–1033.

Siddiqqi, J., and G. Atkinson (2002). Ground motion amplification at rock sites across Canada, as determined from the horizontal-to-vertical component ratio, *Bull. Seismol. Soc. Am.* **92,** 877–884.

Weichert, D. H., R. J. Wetmiller, and P. Munro (1986). Vertical earthquake acceleration exceeding 2 *g*? The case of the missing peak, *Bull. Seismol. Soc. Am.* **76,** 1473–1478.

Wells, D. L., and K. J. Coppersmith (1994). New empirical relationships among magnitude, rupture length, rupture width, rupture area, and surface displacement, *Bull. Seismol. Soc. Am.* **84,** 974–1002.

U.S. Geological Survey
MS 977
345 Middlefield Road
Menlo Park, California 94025
boore@usgs.gov
  (D.M.B.)

EQECAT, Inc.
1030 NW 161st Place
Beaverton, Oregon 97006
kcampbell@eqecat.com
  (K.W.C.)

Department of Earth Sciences
University of Western Ontario
London, Ontario, Canada N6A 5B7
gmatkinson@aol.com
  (G.M.A.)